Cell Reports, Volume *32*

Supplemental Information

AMPAR-Dependent Synaptic Plasticity Initiates Cortical Remapping and Adaptive Behaviors during Sensory Experience

Tiago Campelo, Elisabete Augusto, Nicolas Chenouard, Aron de Miranda, Vladimir Kouskoff, Come Camus, Daniel Choquet, and Frédéric Gambino

Figure S1 | Effect of SWE on L2/3 pyramidal neurons excitability. Related to Figure 1.

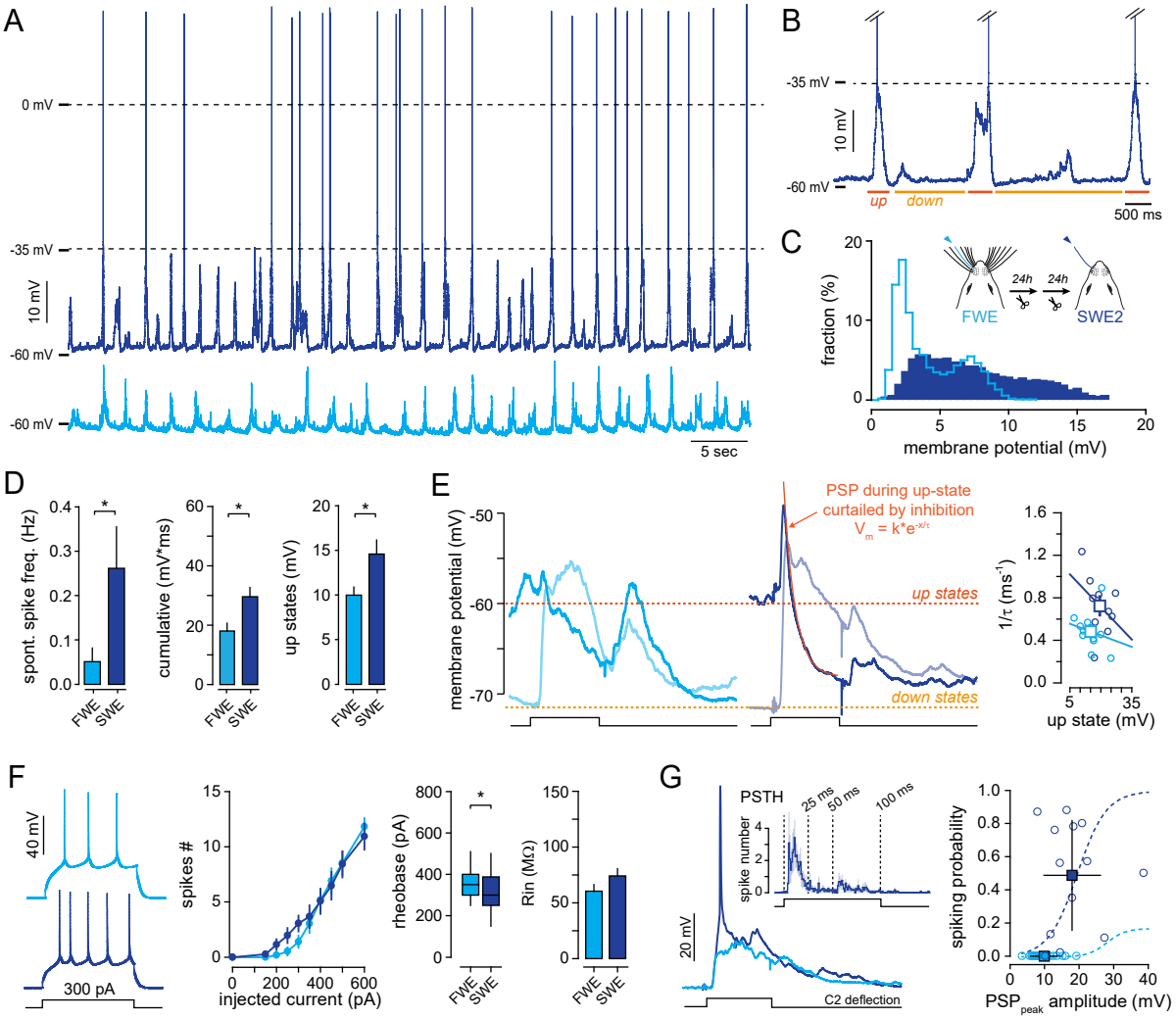

A) Example of two L2/3 S1 pyramidal neurons showing typical spontaneous slow wave fluctuations recorded during FWE (*bottom, light blue*) and SWE (*top, dark blue*). Spontaneous overshooting spikes were observed but only during up states in SWE mice.

B) Same example as in A) but with extended time scale of up (red) and down (orange) states.

C) Spontaneous membrane potential probability histograms for the two cells plotted in A).

D) *Left*, mean (± sem) frequency of spontaneous action potentials. *Middle*, mean (± sem) cumulative spontaneous Vm fluctuations. *Right*, mean (± sem) amplitude of spontaneous up states. FWE, n=9 cells; SWE, n=14 cells.

E) *Left*, PW-evoked PSPs during down (orange) and up (orange) states for both FWE and SWE. Note that a whisker-evoked PSP during up state is rapidly curtailed by synaptic inhibition from intra-cortical circuits. The exponential fit of the decay is an indirect indicative of PW-evoked inhibition into L2/3 pyramidal neurons. *Right*, Scatter plot of the fitted decay as a function of up state amplitude for both FWE and SWE. Squares, averages. Circles, individual cells. FWE, n=13 cells; SWE, n=8 cells.

F) *Left*, example of spiking pattern in FWE and SWE injected mice upon 300pA current injection. *Middle*, average (± sem) number of action potentials (APs) triggered by incremental current injections for both conditions. Median (± interquartile range) minimal current amplitude (pA) triggering action potentials (rheobase, FWE, n=24 cells; SWE, n=27 cells). *Right*, mean (± sem) membrane resistance (Rin, FWE, n=15 cells; SWE, n=12 cells).

G) *Left*, single-cell examples of PW-evoked responses (averaged traces) from FWE and SWE mice. *Insert*, Peristimulus time histograms (PSTH) of whisker-evoked somatic spikes for SWE. Note that the majority of spikes are time-locked to the maximum onset of the whisker-evoked PSP (PSPpeak). *Right*, relationship between PW-evoked PSP amplitude and the spiking probability illustrating the increase in PSP-spike coupling upon SWE. Circles, individual cells (FWE, n=20 cells; SWE, n=13 cells); squares, averages. FWE, light blue; SWE, dark blue.

Figure S2 | Cross-linking GluA2 subunits does not affect circuit spontaneous activity nor whisker-evoked PSP at different holding potentials. Related to Figure 3.

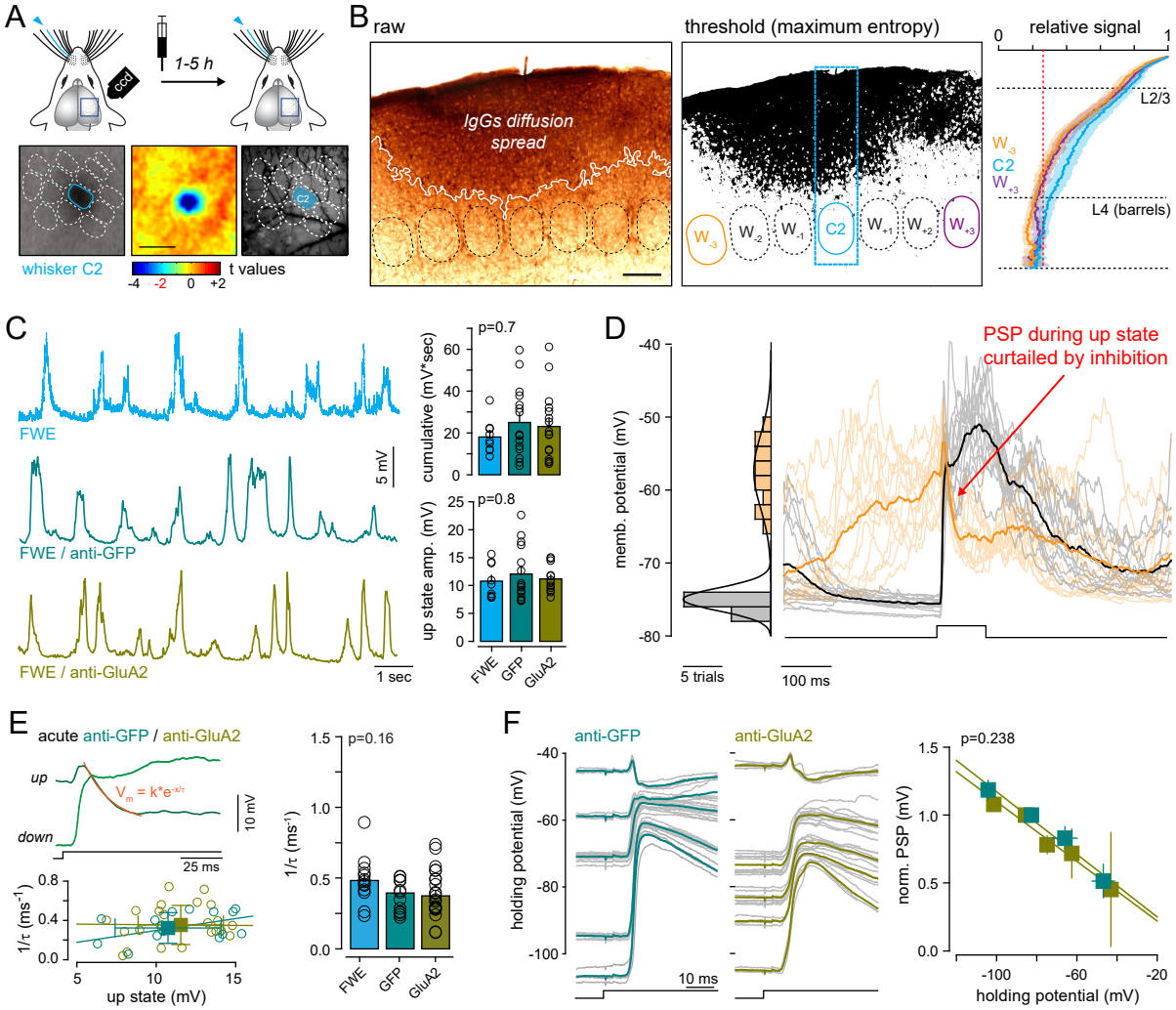

A) Schematic of experimental strategy. IgGs were injected during FWE and targeted to the principal-barrel (C2) using intrinsic optical imaging. Scale bar: 200 µm.

B) *Left*, example of DAB-revealed antibody injection in S1. *Right*, entropy threshold was used to determine antibody diffusion across the barrel column, and barrel field. Note that IgGs are preferentially located in the superficial layers of S1, but present across different barrel columns. Scale bar: 100 µm.

C) *Left*, example of three L2/3 S1 pyramidal neurons showing typical spontaneous slow wave fluctuations recorded during FWE (*top, light blue*), FWE/anti-GFP (*middle, turquoise*), and FWE/anti-GluA2 (*bottom, khaki*. Right, mean (± sem) cumulative Vm fluctuations (mV*sec) and amplitude of up states (mV). Circles, individual cells (FWE, n=9 cells; anti-GFP, n=16 cells; andti-GluA2, n=16 cells).

D) *Left*, membrane potential histogram showing the average (30 ms) membrane potential before each PW stimulation. Down (gray) and up (light orange) states follow separated Gaussian distributions. *Right*, PW-evoked PSP during down (black) and up (orange) states. Individual trials are represented with light lines. Note that whisker-evoked PSP during up state is rapidly curtailed by synaptic inhibition from intra-cortical circuits.

E) *Left top*, single-cell examples of PW-evoked PSP in down and up states. The decay of membrane potential during up states is fitted with an exponential, which is indicative of the amount of PW-evoked inhibition. *Left bottom*, relation between the amplitude of UP states and the exponential tau ($1/\tau$), in anti-GFP (*turquoise*) and anti-GluA2 (*khaki)* IgGs injected mice. Circles, individual cells; squares, mean (± sem). Right, mean (± sem) exponential tau ($1/\tau$) of whisker-evoked inhibition during UP states (mV). Circles, individual cells (FWE, n=13 cells; anti-GFP, n=16 cells; andti-GluA2, n=16 cells).

F) *Left*, single-cells examples of PW-evoked PSPs at different holding potentials. *Right*, relation between holding potential and the amplitude of PW-PSP (normalized to the amplitude at resting membrane potential; anti-GFP, n=4 cells; anti-GluA2, n=2 cells).

Figure S3 | Comparison between all the different treatments for w-Pot, plateau strength and basic cell properties. Related to Figures 4 and 5.

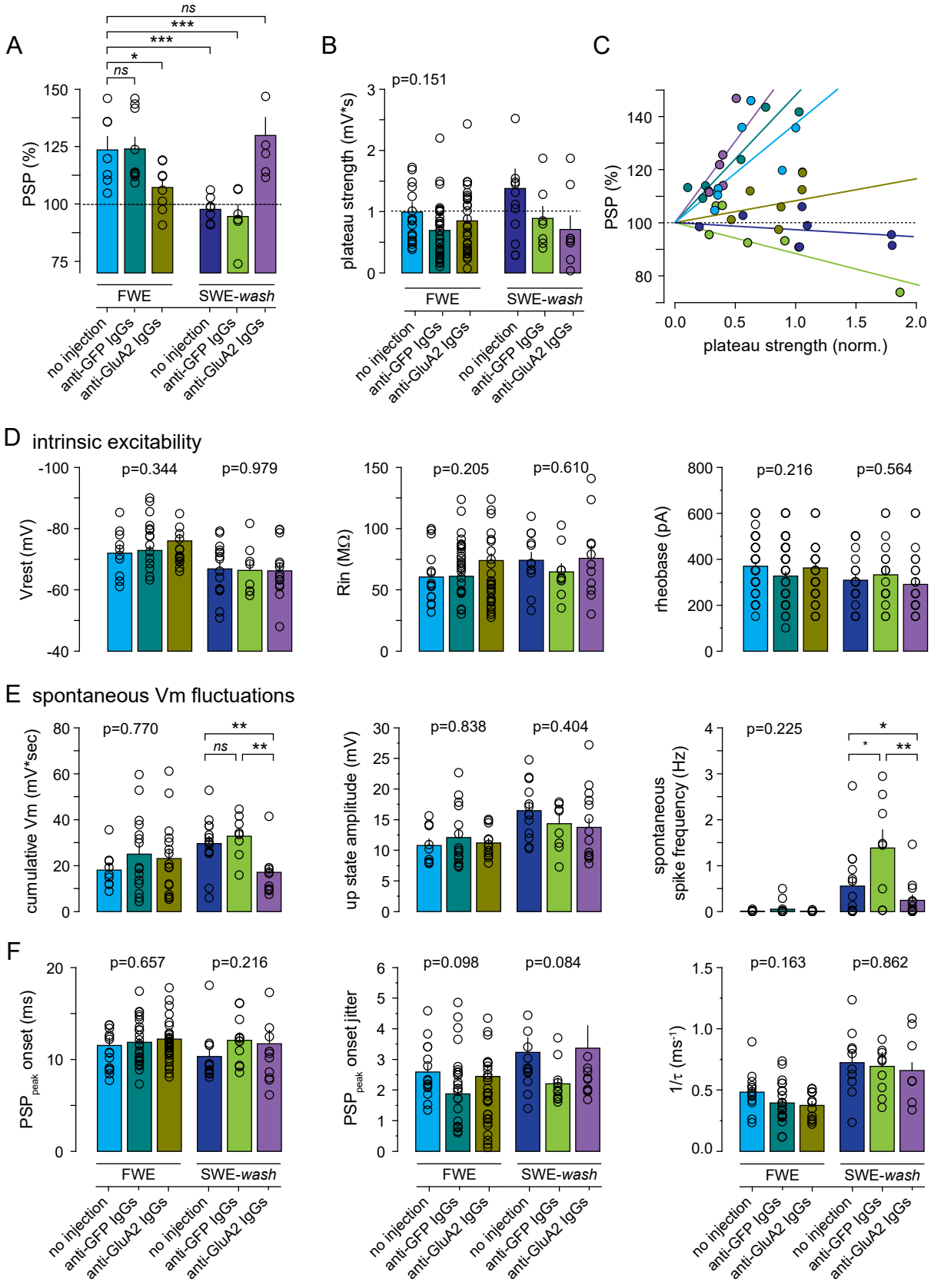

A) Mean (± sem) PSP amplitude normalized to baseline. Circles, individual cells (FWE, no injection n=7; anti-GFP n=9; anti-GluA2 n=8; SWE-wash, no injection n=7, anti-GFP n=6; anti-GluA2 n=6).

B) Mean (± sem) plateau strength. Circles, individual cells (FWE, no injection n=20; anti-GFP n=34; anti-GluA2 n=31; SWE-wash, no injection n=13, anti-GFP n=7; anti-GluA2 n=9).

C) Correlation between normalized plateau strength and the level of RWS-induced w-Pot for all treatments. Only the conditions SWE (dark blue) and FWE+antiGluA2 IgGs (yellow) dissociate the induction from the expression of w-Pot by suppressing w-Pot without affecting plateau strength.

D) Mean (± sem) Vrest (FWE, no injection n=20; anti-GFP n=34; anti-GluA2 n=31; SWE-wash, no injection n=13, anti-GFP n=7; anti-GluA2 n=9), Rin (FWE, no injection n=15; anti-GFP n=28; anti-GluA2 n=28; SWE-wash, no injection n=12, anti-GFP n=9; anti-GluA2 n=11), and rheobase (FWE, no injection n=50; anti-GFP n=38; anti-GluA2 n=64; SWE-wash, no injection n=24, anti-GFP n=20; anti-GluA2 n=22). Circles, individual cells.

E) Mean (± sem) cumulative Vm (FWE, no injection n=9; anti-GFP n=16; anti-GluA2 n=16; SWE-wash, no injection n=14, anti-GFP n=8; anti-GluA2 n=10), up state amplitude (FWE, no injection n=9; anti-GFP n=16; anti-GluA2 n=16; SWE-wash, no injection n=14, anti-GFP n=8; anti-GluA2 n=13), and spontaneous spike frequency (FWE, no injection n=9; anti-GFP n=16; anti-GluA2 n=16; SWE-wash, no injection n=14, anti-GFP n=8; anti-GluA2 n=13). Circles, individual cells.

F) Mean (± sem) PSP onset and onset jitter (FWE, no injection n=15; anti-GFP n=31; anti-GluA2 n=25; SWE-wash, no injection n=12, anti-GFP n=11; anti-GluA2 n=11), and 1/t (see Fig. S1E and S3D, E). Circles, individual cells.

Figure S4 | Short-term dynamics of membrane potential during RWS is not affected by acute nor chronic cross-linking of the GluA2 AMPAR subunit. Related to Figures 4 and **5.**

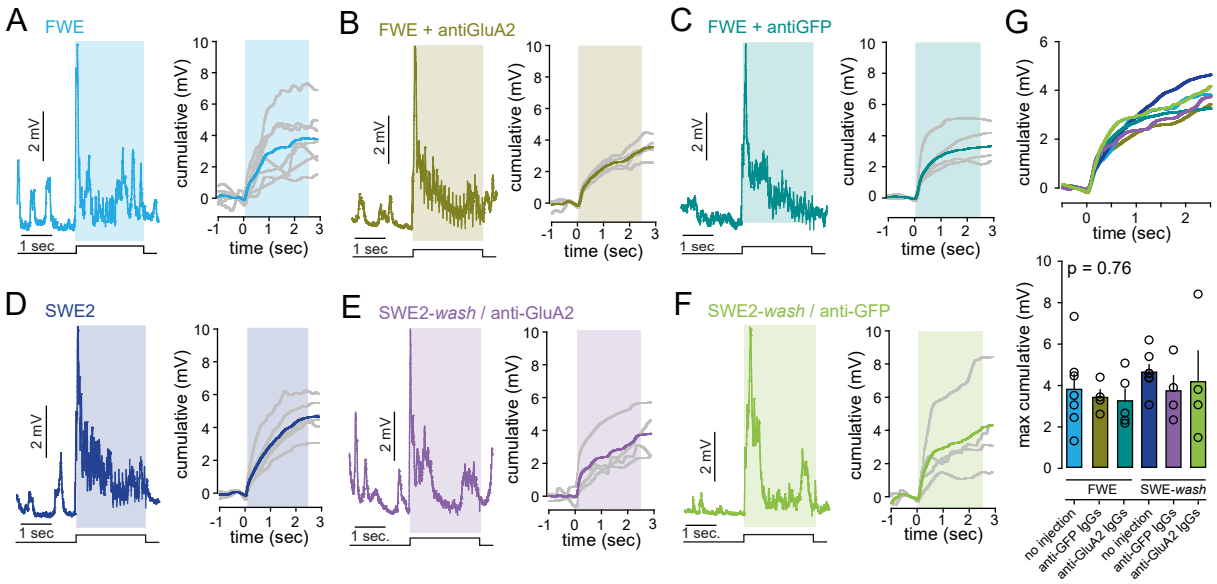

A) *Left*, FWE single-cell average (blue) of the variation on the resting membrane potential (Vm) upon RWS. Square pulse lines, C2 whisker deflection (RWS, 8 Hz during 2.5 sec.). *Right*, grand average of cumulative during RWS. Gray lines, average of each individual cell.

B, C) same than A) but for acute anti-GluA2 (*khaki*), and anti-GFP (*turquoise*) IgGs stereotaxic injections in FWE mice, respectively.

D) Same than A) but for SWE condition.

E, F) same than D) but after chronic injection of GluA2 (magenta) or GFP (light green) IgG stereotaxic injections, respectively.

G) *Top*, average of the cumulative Vm during RWS for all the experimental conditions. *Bottom*, mean (± sem) of the maximum cumulative Vm (at 2.5 sec.) for all the conditions. Circles, individual cells (FWE, no injection n=7; anti-GFP n=4; anti-GluA2 n=5; SWE-wash, no injection n=7, anti-GFP n=4; anti-GluA2 n=4).

Figure S5 | Chronic anti-GluA2 IgG injections do not increase inflammation as compared to anti-GFP IgG injections. Related to Figure 5.

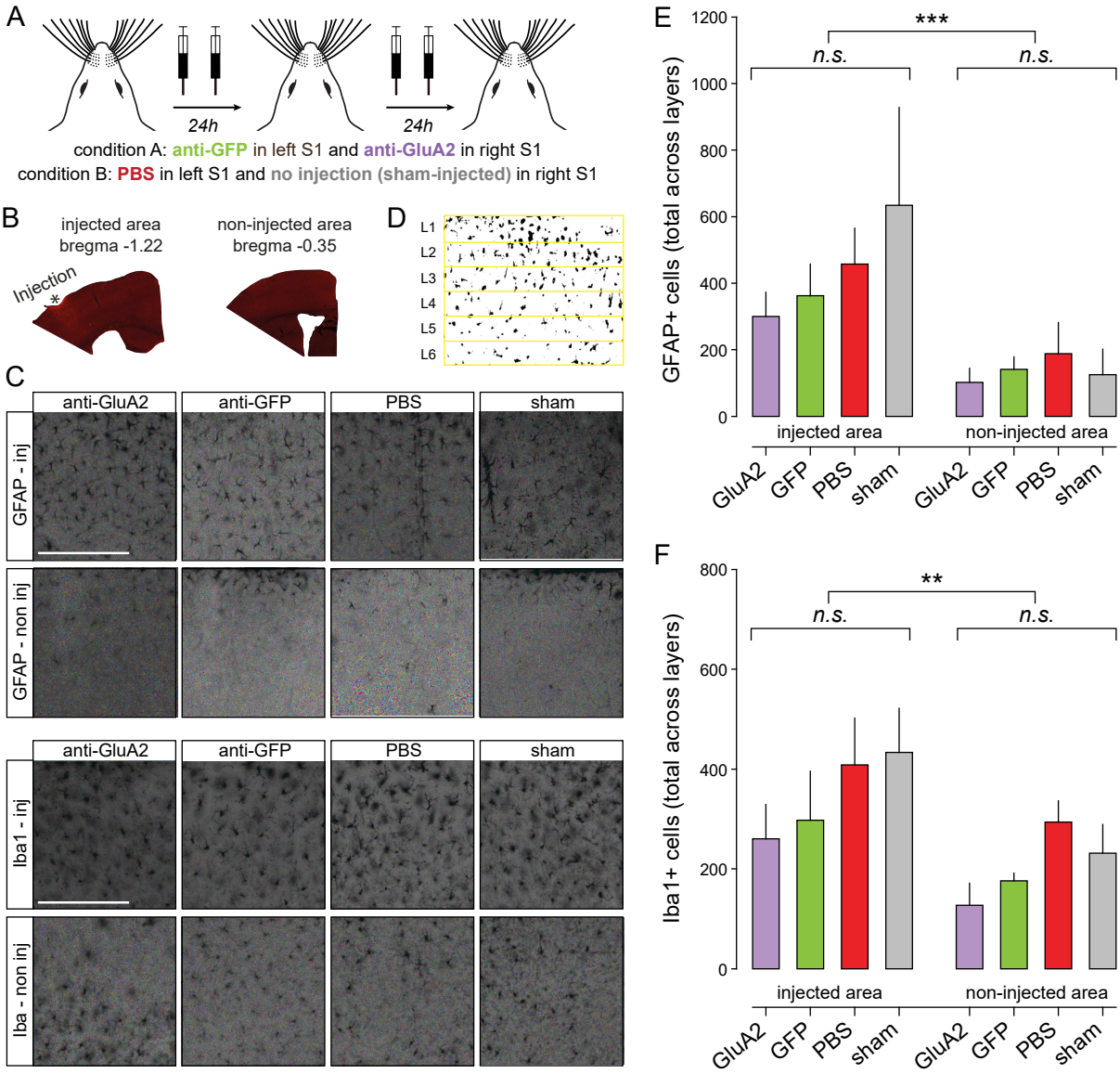

A) Schematic of experimental strategy. Injections were done twice a day for two consecutive days in FWE mice. In a first cohort of mice, anti-GluA2 and anti-GFP IgG were injected in the right and left hemispheres, respectively. A second cohort of mice was used as control, in which PBS was injected in the left hemisphere while only a craniotomy was performed on the right hemisphere with no injection (sham-injected).

B) Immunostaining was quantified in the injected area as well as in cortical area far away from the injection site for control where the presence of IgG is unlikely.

C) Immunostaining examples for the astrocyte marker GFAP (*top*) and the microglia marker Iba1 (*bottom*), for each experimental condition, in the injection site (*inj*) and in cortical area away from the injection site (*non inj*). Scale bars, 200µm.

D) Entropy threshold algorithm was used to determine the number of immunopositive cells across layers**.**

E) Quantification of GFAP immunopositive (GFAP+) cells. Detected cells across cortical layers were pooled together. Mean ± sem. Number of mice: injected area, GluA2: 4, GFP: 4, PBS: 4, sham: 4; non-injected area, GluA2: 5, GFP: 5, PBS: 4, sham: 4.

F) Same presentation as in E) but for the microglia marker Iba1. Number of mice: injected area, GluA2: 5, GFP: 5, PBS: 7, sham: 7; non-injected area, GluA2: 4, GFP: 4, PBS: 6, sham: 6.

Figure S6 | IgGs do not alter exploration and decision latency. Related to Figure 6.

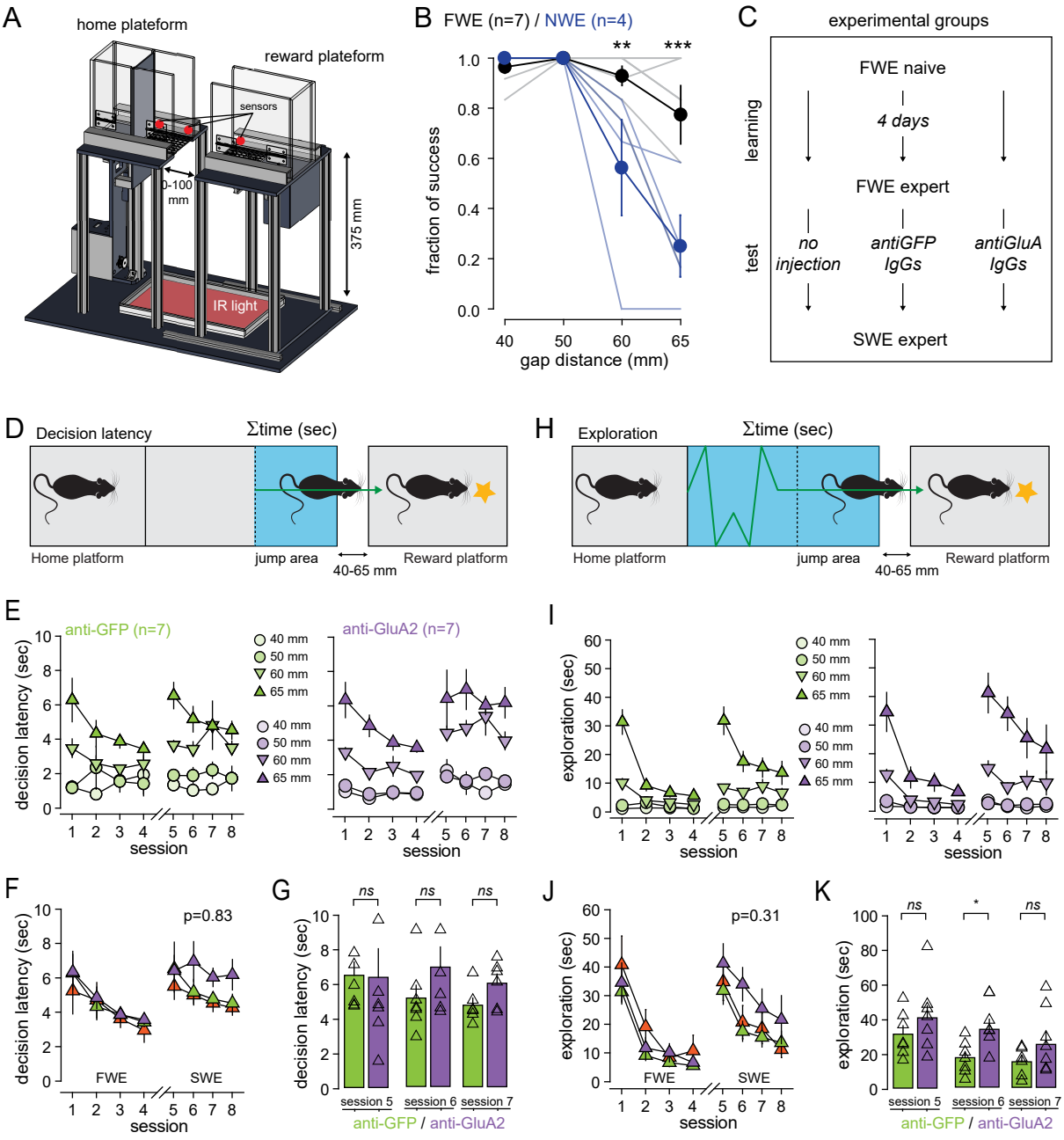

A) Overview of the gap-crossing apparatus. It consists of two individual moveable platforms: (i) a starting platform containing an automated door to precisely control the start of a trial; (ii) a reward platform containing a pellet distributor to deliver a calibrated food reward. Both platforms are elevated 374 mm from the surface and surrounded with 20-cm-high plexiglas walls. The two platforms face each other with an infra-red pad at the bottom. The edges of the platforms close to the gap (10 x 10 cm) are made of a metal grid to allow a better grip during jump. A ruler placed in between the platforms is used to precisely define the gap distances at a given trial. Behavior is done without any sensory cues forcing mice to use their whiskers.

B) Averaged (± sem) fraction of gap-crossing success at a distance of 65 mm, in FWE (black) and fully-deprived (no whiskers, NWE, blue). Gray lines, individual mice (FWE, n=7; NWE, n=4).

C) Behavioral protocol and groups. Food-restricted mice are first habituated to the apparatus. During test, each session consists of 3 blocks of 16 trials with pseudo-randomized gap distance (40, 50, 60, and 65 mm). A given trial is defined as success if mice reach the reward platform and eat the food pellet or as a failure if it takes more than 2 min to do so. At the end each trial, the animal is placed back in the home platform to start the next one. Each session ends with a catch trial where the reward platform is removed. This allows to rule out any motor habituation during jumping decision.

D, H) Behavioral parameters. The total time (∑time, sec) spent in the jump area (light blue in D) and in the apparatus (light blue in **H**, excluding the start zone) are used as metrics for decision latency and exploration, respectively.

E) Averaged (± sem) decision latency (sec) for different gap distances, in anti-GFP (*left*) and anti-GLuA2 (*right*) injected mice.

F) Averaged (± sem) decision latency (sec) at a distance of 65 mm, in non-injected (orange), anti-GFP (green) and anti-GLuA2 (purple) injected mice.

G) Mean (± sem) decision latency (sec) at a distance of 65 mm after expertise in FWE mice and during SWE. Triangles, individual mice (anti-GFP, n=7; anti-GluA2, n=7).

I-K), Same representation as in **E-G** but for exploration.